Rational design of FeO_x-MoP@MWCNTs composite electrocatalysts toward efficient overall water splitting

Aijian Wang[a,*], Xiaoliang Shen[a], Qi Wang[a], Laixiang Cheng[a], Xiaodong Chen[a,*], Cuncai Lv[b,*] Weihua Zhu[a] and Longhua Li[a]

[a] School of Chemistry & Chemical Engineering, Jiangsu University, Zhenjiang 212013, P.R. China

[b] Key Laboratory of High-precision Computation and Application of Quantum Field Theory of Hebei Province, The College of Physics Science and Technology, Hebei University, Baoding 071002, PR China

Corresponding Author. Tel: +86-511-88791928. E-mail: wajujs@ujs.edu.cn, cxdoyy@163.com, lvcuncai@163.com

Experimental section

Reagents and materials

Molybdenum pentachloride ($MoCl_5$), potassium hydroxide (KOH), ferric chloride ($FeCl_3.6H_2O$) and sodium phosphate ($NaH_2PO_4.2H_2O$) were obtained from Sinopharm Chemical Reagent Co., Ltd. MWCNTs were purchased from Beijing DK Nano Technology and used as received. The deionized water used in all experimental processes was obtained through an Ulupure system.

Physicochemical characterization

The morphologies, composition and structure of the as-prepared samples were investigated by the X-ray diffraction (XRD) pattern (a XD-3 diffractometer with Cu Ka radiation), Raman spectra (a Renishaw Invia Raman Microscope), scanning electron microscopy (SEM, a Model S4800, Hitachi), X-ray photoelectron spectroscopy (XPS, a RBD upgraded PHI-5000C ESCA), transmission electron microscopy (TEM, a JEM-2100 HR, JEOL system) and Brunauer-Emmett-Teller (BET) specific surface areas (a Quantachrome Nove 2000e sorption analyzer).

Electrochemical measurements

All electrochemical measurements were performed on a CHI 614E

electrochemical workstation (CH Instrument, China) in 1.0 M KOH solution with a scan rate of 2 mV/s. The sample covered glassy carbon electrode with 3 mm diameter is employ as the working electrode, a Pt gauze (1 × 1 cm^2) as the counter electrode and a mercury/ mercury oxide electrode (MOE) as the reference electrode. The long-term stability of the samples was also examined by using the same electrolyzer. To prepare the working electrode, the catalysts (2 mg) and Nafion solution (5wt%, 40 μL) were dispersed in CH_3CH_2OH (0.5 mL), then the solution was sonicated for 1.0 h to give the homogeneous ink. Subsequently, the well-mixed suspension (15μL) was loaded onto the polished glassy carbon electrode. The obtained electrode was then dried naturally at room temperature and retained for use. The measured potential in this work has been calibrated with the reversible hydrogen electrode potential (RHE) based on Nernst equations. The electrochemical impedance spectroscopy (EIS) measurement was recorded in the frequencies ranging from 0.01 Hz to 100 KHz with an amplitude of 1 mV. The double-layer capacitance of the as-synthesized samples is determined by the cyclic voltammograms with different scan rates (20, 40, 60, 80, and 100 mV/s) in the scope of 0.1-0.2 V *vs.* RHE.

Preparation of FeO_x-MoP@MWCNTs composite electrocatalysts

In a typical synthetic route to prepare FeO_x-MoP@MWCNTs composite electrocatalysts, a certain amount of $FeCl_3.6H_2O$, $MoCl_5$ (30 mg), NaH_2PO_4 (120 mg), polyvinylpyrrolidone (30 mg) and MWCNTs (5 mg) were added into deionized water (50 mL) to form a homogeneous aqueous solution by ultrasonic treatment. Solid powder was obtained by removing the solvent under 60 ^oC. Then, the powder was calcined at 750 ^oC for 5 h with a heating rate of 10 $^oC\ min^{-1}$ under N_2 flow to generate FeO_x-MoP@MWCNT composite electrocatalysts. In the present case, the amount of $MoCl_5$ was fixed while the content of $FeCl_3.6H_2O$ is varied. The samples with different $FeCl_3.6H_2O$:$MoCl_5$ mass ratios of 1:15, 2:15 and 3:15 are denoted as FeO_x-MoP@MWCNT-1, FeO_x-MoP@MWCNT-2 and FeO_x-MoP@MWCNT-3, respectively. For comparison, the FeO_x-MoP was also fabricated in the same way to FeO_x-MoP@MWCNT composite electrocatalysts, just without adding MWCNTs.

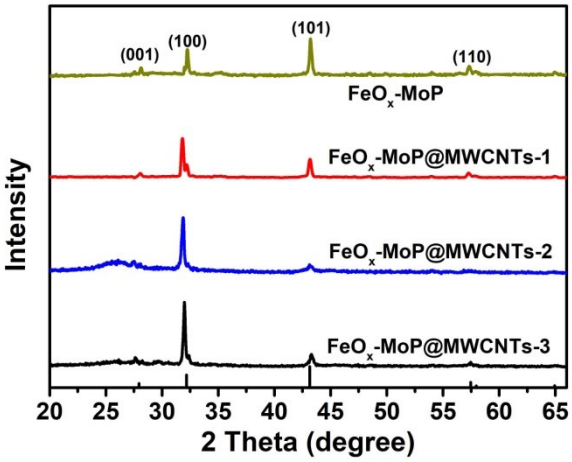

Figure S1. XRD patterns of the as-prepared samples.

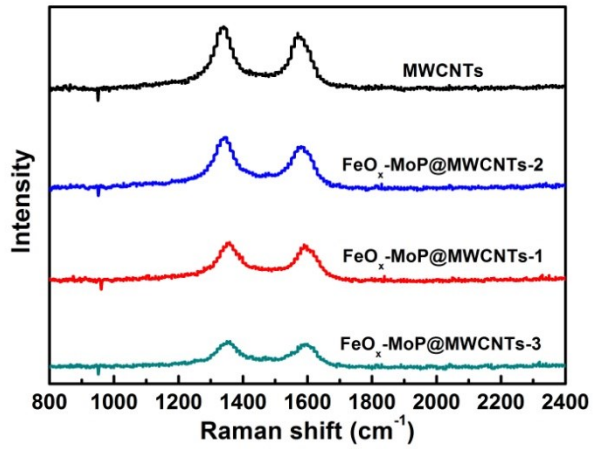

Figure S2. Raman spectra of the as-prepared samples.

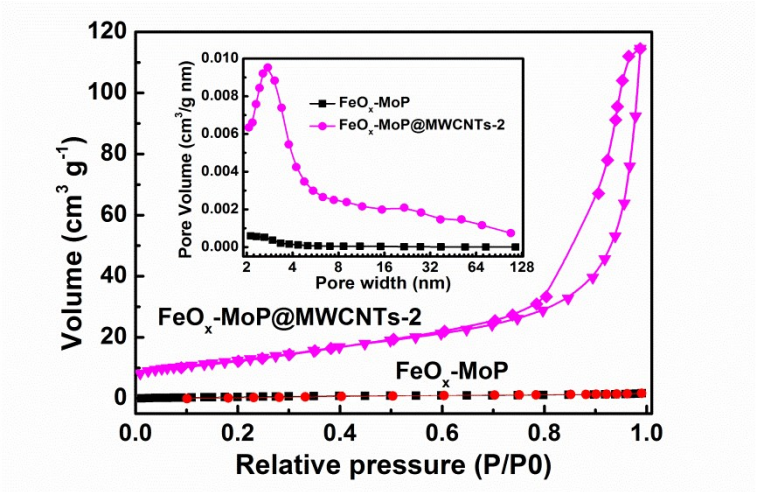

Figure S3. Nitrogen adsorption-desorption isotherms of FeO_x-MoP and FeO_x-MoP@MWCNTs-2 (Inset is the pore distribution of above two samples.)

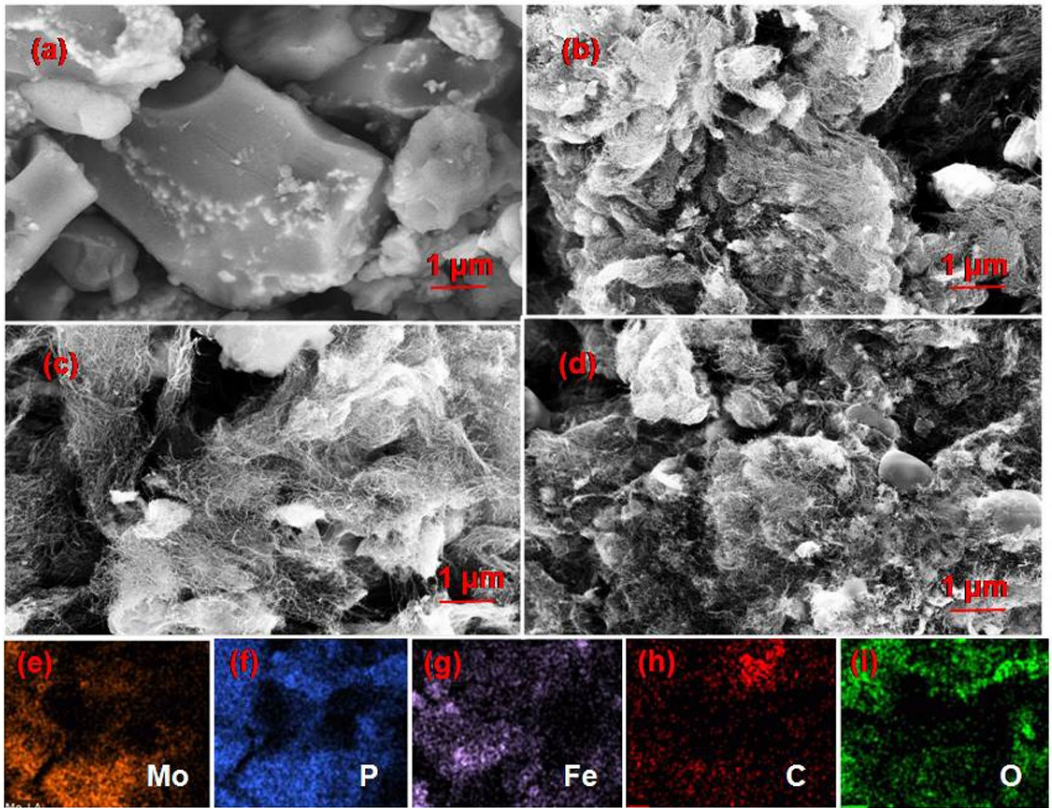

Figure S4. SEM images of (a) FeO_x-MoP, (b) FeO_x-MoP@MWCNTs-1, (c) FeO_x-MoP@MWCNTs-2 and (d) FeO_x-MoP@MWCNTs-3; and elemental mapping images of (e) Mo, (f) P, (g) Fe, (h) C and (i) O for FeO_x-MoP@MWCNTs-2.

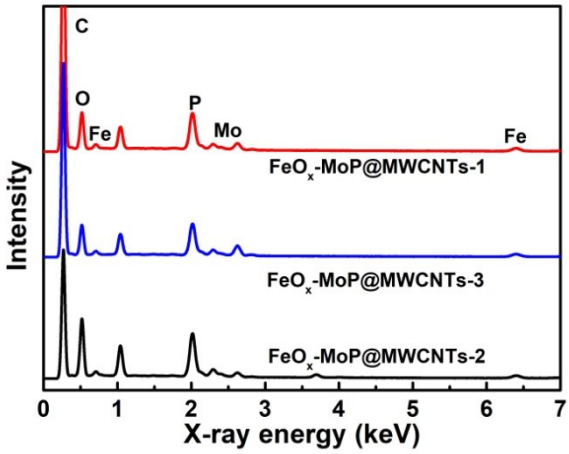

Figure S5. The energy-dispersive X-ray spectra of the as-prepared samples.

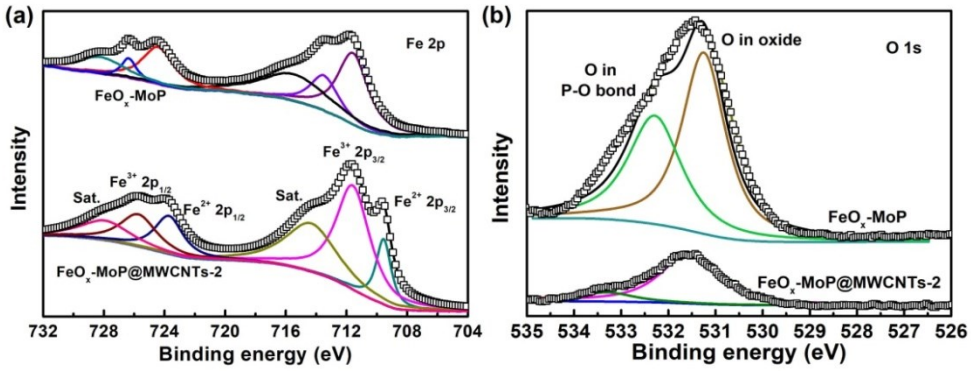

Figure S6. High-resolution XPS spectra of (a) Fe 2p and (b) O 1s.

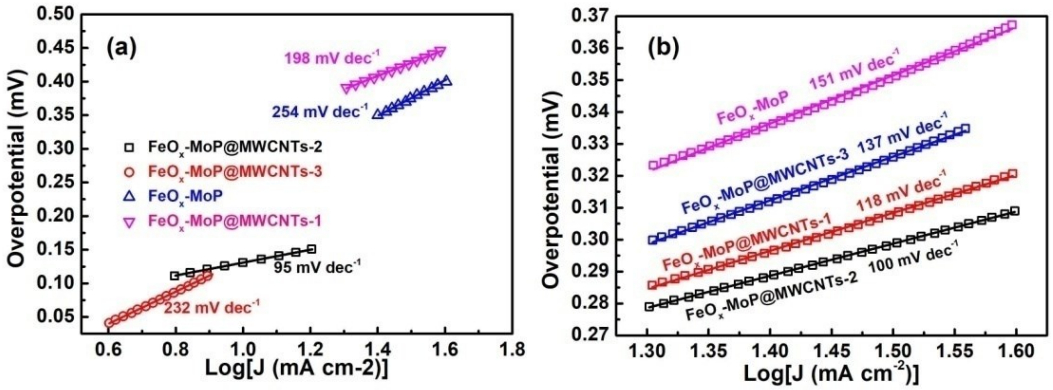

Figure S7. Tafel plots of the as-prepared samples derived from (a) HER and (b) OER LSV curves.

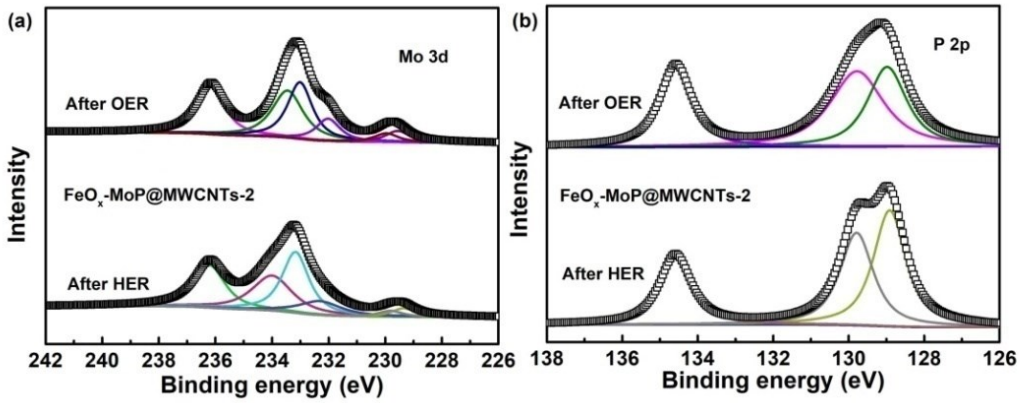

Figure S8. High resolution XPS spectra of FeO_x-MoP@MWCNTs-2 in the regions of (a) Mo 3d and (b) P 2p after HER and OER measurements.

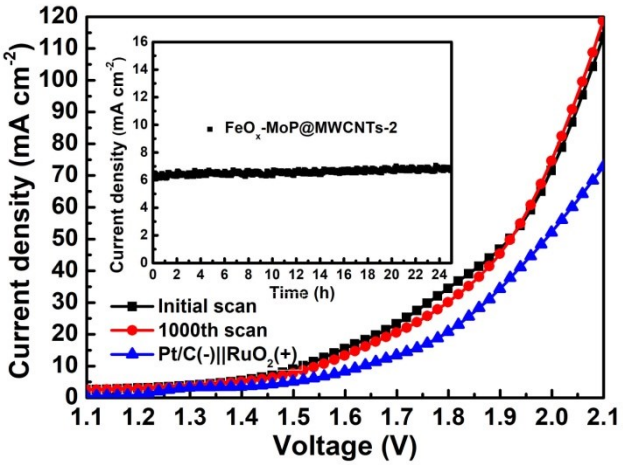

Figure S9. Overall water splitting performance of FeO_x-MoP@MWCNTs-2 and Pt/C(-) ‖ RuO_2(+) cell. Inset is the catalytic stability of FeO_x-MoP@MWCNTs-2 in 1.0 M KOH.

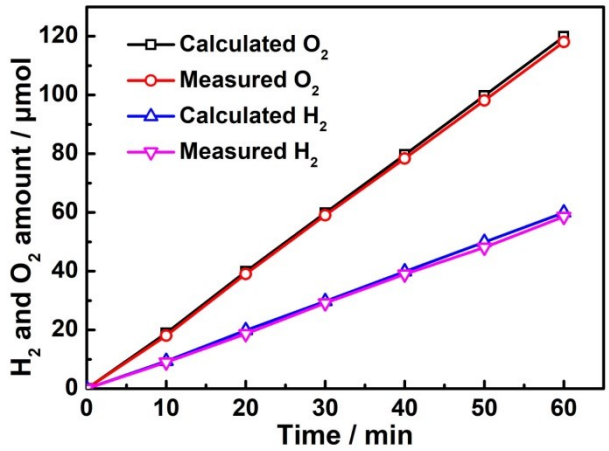

Figure S10. The amount of H_2 and O_2 experimentally measured and theoretically calculated as a function of time for FeO_x-MoP@MWCNTs-2.

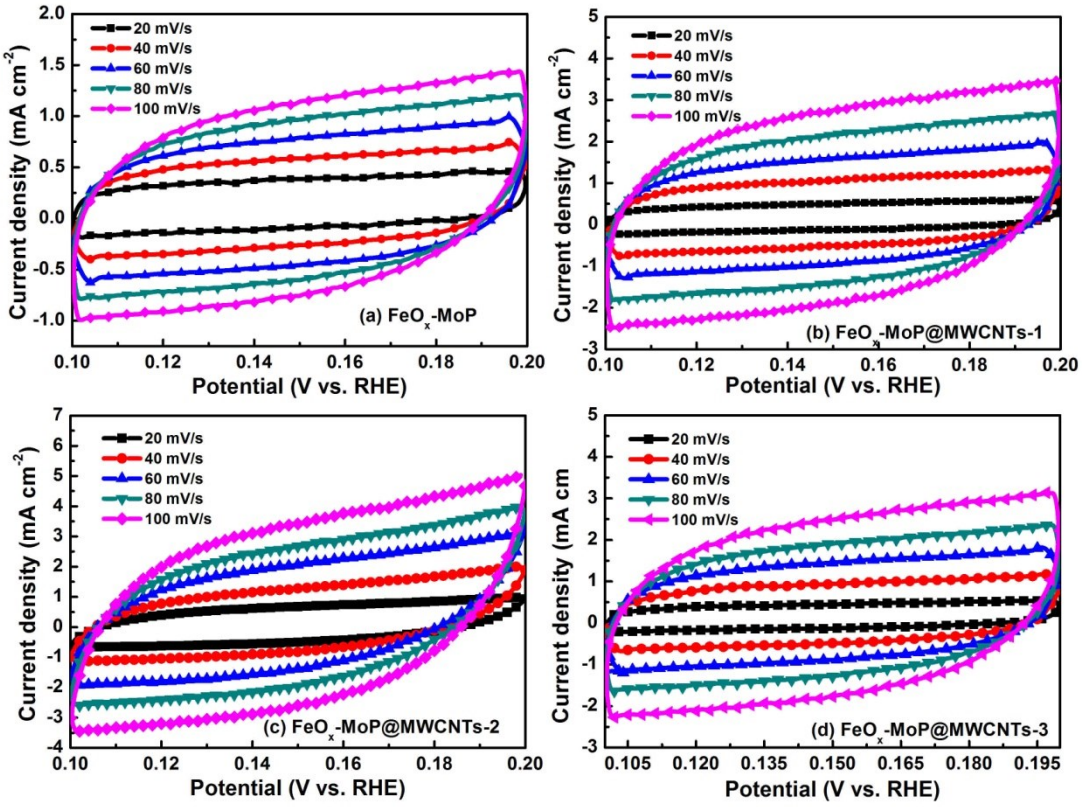

Figure S11. Cyclic voltammograms of (a) FeO_x-MoP, (b) FeO_x-MoP@MWCNTs-1, (c) FeO_x-MoP@MWCNTs-2 and (d) FeO_x-MoP@MWCNTs-3.

Computational method

We have employed the first-principles [1,2] to perform all Spin-polarization density functional theory (DFT) calculations within the generalized gradient approximation (GGA) using the Perdew-Burke-Ernzerhof (PBE) [3] formulation. We have chosen the projected augmented wave (PAW) potentials [4,5] to describe the ionic cores and take valence electrons into account using a plane wave basis set with a kinetic energy cutoff of 350eV. Partial occupancies of the Kohn-Sham orbitals were allowed using the Gaussian smearing method and a width of 0.06 eV. The electronic energy was considered self-consistent when the energy change was smaller than 10^{-5} eV. A geometry optimization was considered convergent when the energy change was smaller than 0.05 eV $Å^{-1}$. In addition, for the Fe atoms, the U schemes need to be applied, and the U has been set as 3.2 eV. The solvation model has been used in our calculation. The free energy was calculated using the equation:

$$G = E + ZPE - TS$$

where G, E, ZPE and TS are the free energy, total energy from DFT calculations, zero point energy and entropic contributions (T was set to be 300K), respectively.

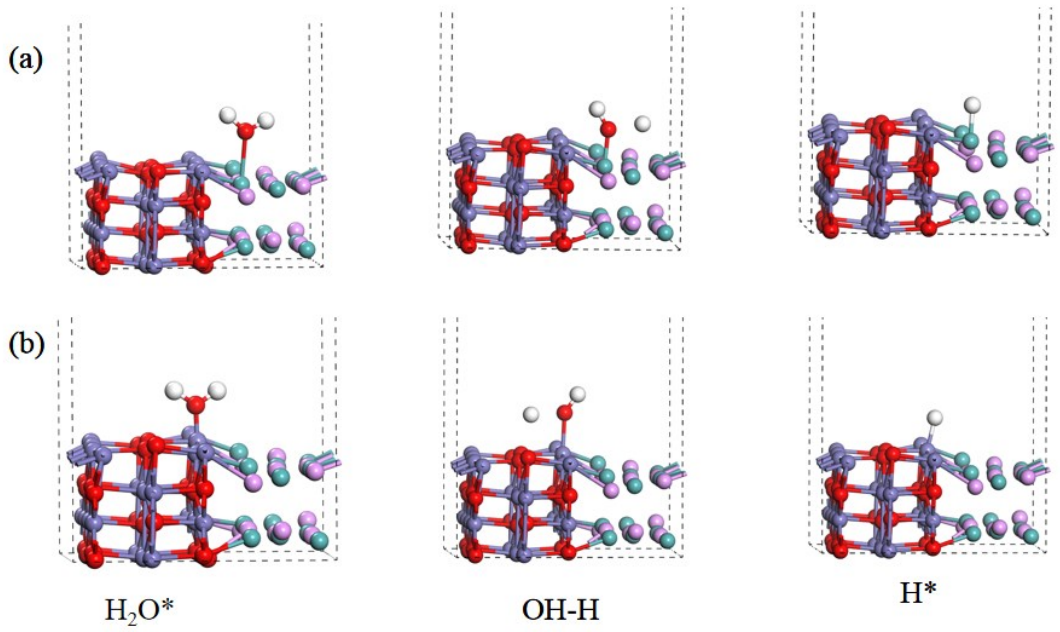

Figure S12. DFT-optimized structures of FeO_x-MoP for HER: (a) Mo sites and (b) Fe sites.

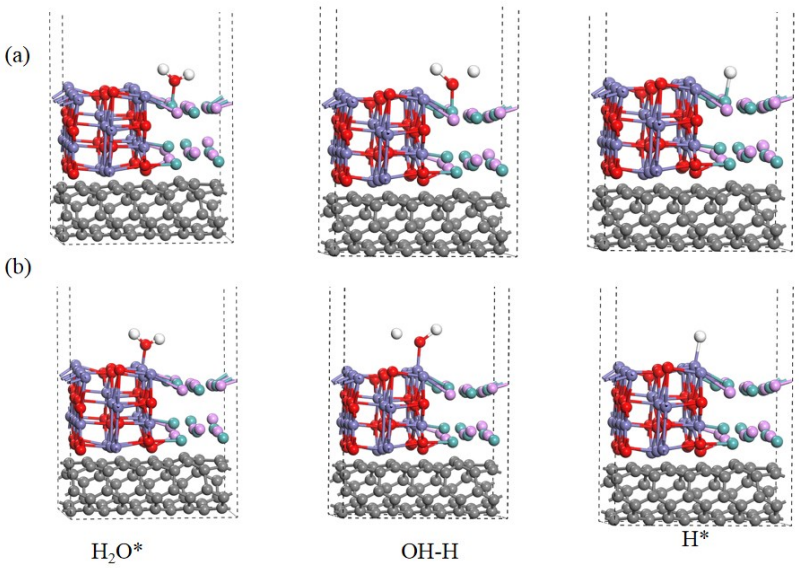

Figure S13. DFT-optimized structures of FeO_x-MoP@MWCNTs-2 for HER: (a) Mo sites and (b) Fe sites.

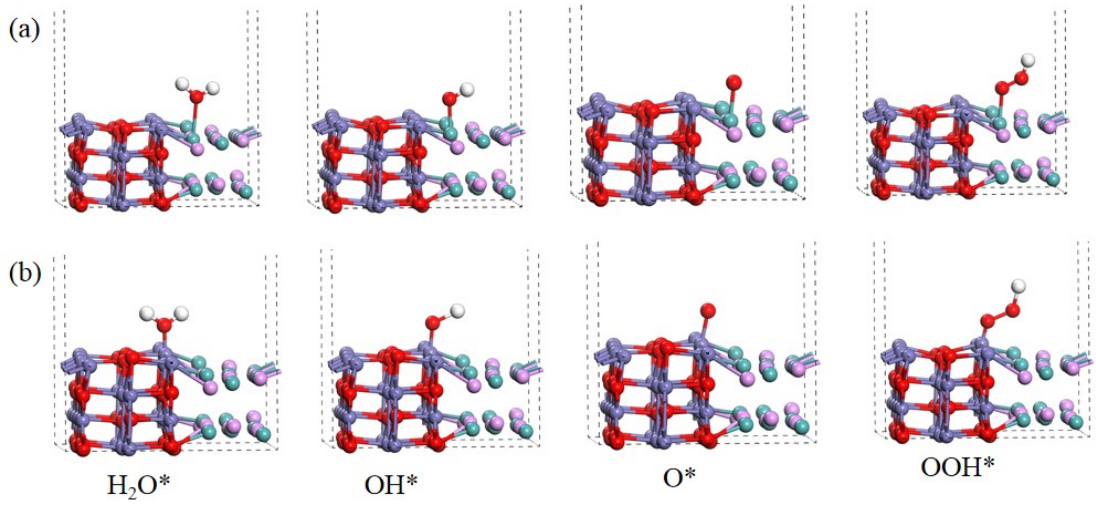

Figure S14. DFT-optimized structures of FeO_x-MoP for OER: (a) Mo sites and (b) Fe sites.

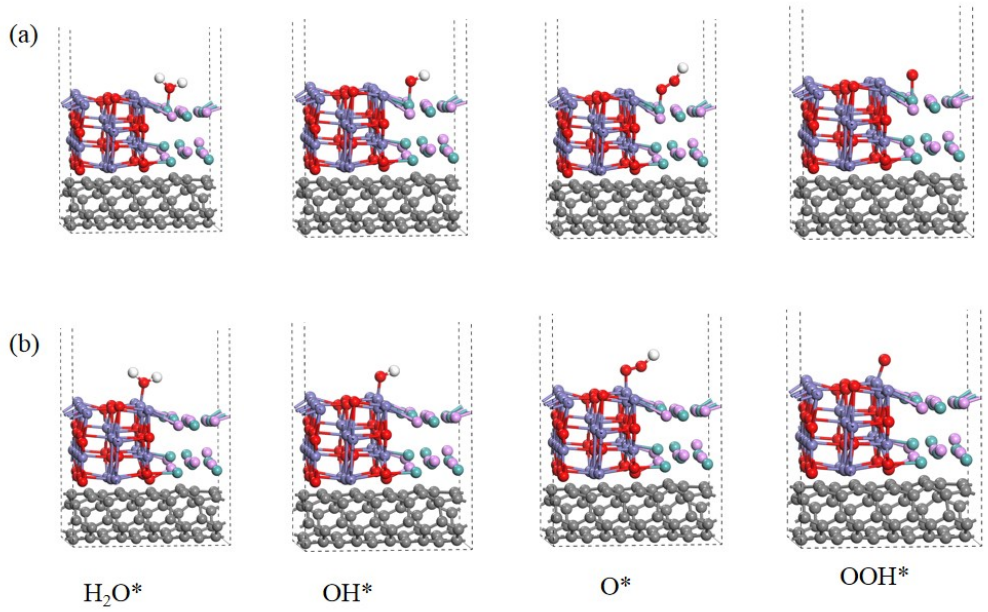

Figure S15. DFT-optimized structures of FeO_x-MoP@MWCNTs-2 for OER: (a) Mo sites and (b) Fe sites.

Table S1. Comparison of HER performance of FeO_x-MoP@MWCNTs-2 with some other reported electrocatalysts.

Electrocatalysts	**Overpotential (mV@10 mA cm^{-2})**	**Ref.**
FeO_x/FeP	96 (1.0 M KOH)	6
CoP_3/CoMoP-5/NF	110 (1.0 M KOH)	7
MoP/Ni_2P	100.2 (1.0 M KOH)	8
MoP nanoflakes/NF	114 (1.0 M KOH)	9
FeMoP-0.10	195 (1.0 M KOH)	10
MoP@NC-MF	125 (0.5 M H_2SO_4)	11
MoP NTs/Mo	269 (1.0 M KOH)	12
MoPS/NC	170 (1.0 M KOH)	13
MoP@NPCS	113 (0.5 M H_2SO_4)	14
NiFeP@C	160 (1.0 M KOH)	15
MoP@NCHSs-900	92 (1.0 M KOH)	16
MoC-MoP/BCNC NFs	137 (1.0 M KOH)	17
MoP@NCF	129.5 (1.0 M KOH)	18
MoP@NCF	234.6 (0.5 M H_2SO_4)	19
Hierarchical MoP/NF	114 (1.0 M KOH)	20
CoP(MoP)-$CoMoO_3$@CN	198 (1.0 M KOH)	21
MoP-RGO-0.5	152 (1.0 M KOH)	22
MnP-MoP NPs/N,P-Gr	74.2 (1.0 M KOH)	23
MoS_2-MoP-CNS	93 (1.0 M KOH)	24
MoS_2-MoP/C	102 (0.5 M H_2SO_4)	25
Defects-rich MoP/C	100 (1.0 M KOH)	26
MoP-RGO	117 (0.5 M H_2SO_4)	27
FeO_x-MoP/MWCNTs-2	**78**	**This work**

Table S2. Comparison of OER performance of FeO_x-MoP@MWCNTs-2 with other reported electrocatalysts in alkaline electrolyte.

Electrocatalysts	Overpotential (mV@10 mA cm^{-2})	Ref.
MoP nanoflakes/NF	265	9
NiFeP@C	260	15
Hierarchical MoP/NF	265	20
CoP(MoP)-$CoMoO_3$@CN	296	21
FeCo/SWCNT	253	28
Co/Co_9S_8@SNGS-1000	290	29
Co_9S_8@NOSC-900	340	30
Ni_3S_2@$Co(OH)_2$	257	31
$Mo_{5.9}Ni_{94.1}S$/NF	213	32
NiFe/ Co_9S_8/Carbon Cloth	219	33
Co@Co_9S_8	285	34
$CoFe_2O_4$@NF	250	35
$Ni_1Co_1O_2$ NWs	248	36
$NiCo_2O_4$@$CoMoO_4$/NF	265 (20)	37
FeO_x-MoP/MWCNTs-2	**229**	**This work**

Table S3. Comparison of the overall water splitting performance of FeO_x-MoP@MWCNTs-2 with other reported electrocatalysts in alkaline electrolyte.

Electrocatalysts	Cell voltage (V@10 mA cm^{-2})	Ref.
MoP/Ni_2P	1.55	8
Hierarchical MoP/NF	1.62	20
CoP(MoP)-$CoMoO_3$@CN	1.55	21
Co/Co9S8@SNGS-1000	1.58	29
Co_9S_8@NOSC-900	1.60	30
Ni_3S_2@$Co(OH)_2$	1.61	31
$Mo_{5.9}Ni_{94.1}S$/NF	1.485	32
$Ni_1Co_1O_2$ NWs	1.58	36
$NiCo_2O_4$@$CoMoO_4$/NF	1.55	37
CoP@NPCSs	1.64	38
Fe-CoP/Ti	1.60	39
Oxidized CoP	1.59	40
Mo-doped CoP	1.57	41
Pt/C(-) ‖ RuO_2 (+)	1.63	21
FeO_x-MoP/MWCNTs-2	**1.51**	**This work**

References

[1] G. Kresse, J. Furthmüller, Efficiency of Ab-Initio Total Energy Calculations for Metals and Semiconductors Using a Plane-Wave Basis Set, *Comput. Mater. Sci.*, 1996, **6**, 15-50.

[2] G. Kresse, J. Furthmüller, Efficient Iterative Schemes for Ab Initio Total-Energy Calculations Using a Plane-Wave Basis Set, *Phys. Rev. B*, 1996, **54**, 11169-11186.

[3] J. P. Perdew, K. Burke, M. Ernzerhof, Generalized Gradient Approximation Made Simple, *Phys. Rev. Lett.*, 1996, **77**, 3865-3868.

[4] G. Kresse, D. Joubert, From Ultrasoft Pseudopotentials to the Projector Augmented-Wave Method, *Phys. Rev. B*, 1999, **59**, 1758-1775.

[5] P. E. Blöchl, Projector Augmented-Wave Method, *Phys. Rev. B*, 1994, **50**, 17953-17979.

[6] J. W. Huang, Y. Su, Y. D. Zhang, W. Q. Wu, C. Y. Wu, Y. H. Sun, R. F. Lu, G. F. Zou, Y. R. Li, J. Xiong, FeO_x/FeP hybrid nanorods neutral hydrogen evolution electrocatalysis: insight into interface, *J. Mater. Chem. A*, 2018, **6**, 9467-9472.

[7] D. L. Jiang, Y. Xu, R. Yang, D. Li, S. C. Meng, M. Chen, CoP_3/CoMoP heterogeneous nanosheet arrays as robust electrocatalyst for pH-universal hydrogen evolution reaction, *ACS Sustain. Chem. Eng.*, 2019, **7(10)**, 9309-9317.

[8] C. C. Du, M. X .Shang, J. X. Mao, W. B. Song, Hierarchical MoP/Ni_2P heterostructures on nickel foam for efficient water splitting, *J. Mater. Chem. A*, 2017, **5(30)**, 15940-15949.

[9] M. Wang, C. Ye, M. Xu, S. Bao, MoP nanoparticles with a P-rich outermost atomic layer embedded in N-doped porous carbon nanofibers: Self-supported electrodes for efficient hydrogen generation, *Nano Res.*, 2018, **11**, 4728-4734.

[10] X. Liang, D. Z. Zhang, Z. Z. Wu, D. Z. Wang, The Fe-promoted MoP catalyst with high activity for water splitting, *Appl. Catal. A: Gen.*, 2016, **524**, 134-138.

[11] Z. Y. Guo, P. Liu, J. Liu, F. L. Du, L. H. Jiang, Neural network inspired design of highly active and durable N-doped carbon interconnected molybdenum phosphide for hydrogen evolution reaction, *ACS Appl. Energy Mater.*, 2018, **1**, 5437-5445.

[12] H.N. Yu, S. Cao, B. Fu, Z. J. Wu, J. J. Liu, L. Y. Piao, Self-supported nanotubular MoP electrode for highly efficient hydrogen evolution via water splitting, *Catal. Commun.*, 2019, **127**, 1-4.

[13] Y. Huang, X. N. Song, J. Deng, C. Y. Zha, W. J. Huang, Y. L. Wu, Y. G. Li, Ultra-dispersed molybdenum phosphide and phosphosulfide nanoparticles on hierarchical carbonaceous scaffolds for hydrogen evolution electrocatalysis, *Appl. Catal. B: Environ.*, 2019, **245**, 656-661.

[14] J. T. Ren, L. Chen, D. D. Yang, Z. Y. Yuan, Molybdenum-based nanoparticles (Mo_2C, MoP and MoS_2) coupled heteroatoms-doped carbon nanosheets for efficient hydrogen evolution reaction, *Appl. Catal. B: Environ.*, 2020, **263**, 118352.

[15] Q. L. Kang, M. Y. Li, J. W. Shi, Q. Y. Lu, F. Gao, A universal strategy for carbon-supported transition metal phosphides as high-performance bifunctional electrocatalysts towards efficient overall water splitting, *ACS Appl. Mater. Interfaces*, 2020, **12**, 19447-19456.

[16] D. Zhao, K. Sun, W. C. Cheong, L. R. Zheng, C. Zhang, S. J. Liu, X. Cao, K. L. Wu, Y. Pan, Z. W. Zhuang, B. T. Hu, D. S. Wang, Q. Peng, C. Chen, Y. D. Li,

Synergistically interactive pyridinic-N–MoP sites: Identified active centers for enhanced hydrogen evolution in alkaline solution, *Angew. Chem. Int. Ed.*, 2020, **59**, 8982-8990.
[17] N. N. Chen, Q. J. Mo, L. Q. He, X. Q. Huang, L. C. Yang, J. C. Zeng, Q. S. Gao, Heterostructured MoC-MoP/N-doped carbon nanofibers as efficient electrocatalysts for hydrogen evolution reaction, *Electrochim. Acta*, 2019, **299**, 708-716.
[18] X. K. Huang, X. Wang, P. B. Jiang, K. Lan, J. H. Qin, L. Gong, K. Z. Wang, M. Yang, L. Ma, R. Li, Ultrasmall MoP embraced in nitrogen-doped carbon hybrid frameworks for highly efficient hydrogen evolution reaction in both acid and alkaline solutions, *Inorg. Chem. Front.*, 2019, **6**, 1482-1489.
[19] J. S. Li, J. Y. Li, X. R. Wang, S. Zhang, J. Q. Sha, G. D. Liu, Reduced graphene oxide-supported MoP@P-doped porous carbon nano-octahedrons as high-performance electrocatalysts for hydrogen evolution, *ACS Sustainable Chem. Eng.*, 2018, **6**, 10252-10259.
[20] Y. Y. Jiang, Y. Z. Lu, J. Y. Lin, X. Wang, Z. X. Shen, A hierarchical MoP nanoflake array supported on Ni foam: A bifunctional electrocatalyst for overall water splitting, *Small Methods*, 2018, **2**, 1700369.
[21] L. Yu, Y. Xiao, C. L. Luan, J. T. Yang, H. Y. Qiao, Y. Wang, X. Zhang, X. P. Dai, Y. Yang, H. H. Zhao, Cobalt/molybdenum phosphide and oxide heterostructures encapsulated in N-doped carbon nanocomposite for overall water splitting in alkaline media, *ACS Appl. Mater. Interfaces*, 2019, **11**, 6890-6899.
[22] Z. X. Wu, M. Song, Z. J. Zhang, J. Wang, X. Liu, Various strategies to tune the electrocatalytic performance of molybdenum phosphide supported on reduced grapheme oxide for hydrogen evolution reaction, *J. Colloid Interf. Sci.*, 2019, **536**, 638-645.
[23] C. D. Nguyen, V. H. Nguyen, T. Y. Vu, L. M. T. Pham, K. L. Vu-Huynh, Efficient and stable hybrid electrocatalyst of mixed MnP-MoP nanoparticles-N,P-codoped graphene for hydrogen evolution reaction, *Colloid. Surf. A*, 2020, **593**, 124609.
[24] Z. X. Wu, M. Song, X. Liu, Nitrogen doped holey carbon with MoS_2-MoP nanosheets for efficient hydrogen evolution reaction in alkaline medium, *J. Electrochem. Soc.*, 2018, **165**, F976-F980.
[25] Z. X. Wu, J. Wang, K. D. Xia, W. Lei, X. Liu, D. L. Wang, MoS_2-MoP heterostructured nanosheets on polymer-derived carbon as an electrocatalyst for hydrogen evolution reaction, *J. Mater. Chem. A*, 2018, **6**, 616-622.
[26] B. T. Liu, J. Wang, D. D. Wang, J. C. Fu, W. B. Chen, Z. J. Fu, Q. P. Qiang, L. L. Peng, L. Zhao, J. M. Wei, J. B. Qiu, C. G. Ma, The mechanism and surface engineering of carbon encapsulate defects-rich molybdenum phosphide for the hydrogen evolution reaction in alkaline media, *J. Alloys Compd.*, 2021, **850**, 156737.
[27] Z. X. Wu, J. Wang, J. Zhu, J. P. Guo, W. P. Xiao, C. J. Xuan, W. Lei, D. L. Wang, Highly efficient and stable MoP-RGO nanoparticles as electrocatalysts for hydrogen evolution, *Electrochim. Acta*, 2017, **232**, 254-261.
[28] D. Y. Xie, Y. Chen, D. S. Yu, S. L. Han, J. N. Song, Y. Y. Xie, F. Hu, L. L. Li, S. J. Peng, Single-layer carbon-coated FeCo alloy nanoparticles embedded in single-walled carbon nanotubes for high oxygen electrocatalysis, *Chem. Commun.*, 2020, **56**, 6842-6845.
[29] X. Zhang, S. W. Liu, Y. P. Zang, R. R. Liu, G. Q. Liu, G. Z. Wang, Y. X. Zhang, H. M. Zhang, H. J. Zhao, Co/Co_9S_8@S,N-doped porous graphene sheets derived

from S, N dual organic ligands assembled Co-MOFs as superior electrocatalysts for full water splitting in alkaline media, *Nano Energy*, 2016, **30**, 93-102.

[30] S. C. Huang, Y. Y. Meng, S. M. He, A. Goswami, Q. L. Wu, J. H. Li, S. F. Tong, T. Asefa, M. M. Wu, N-, O-, and S-Tridoped carbon-encapsulated Co_9S_8 nanomaterials: Efficient bifunctional electrocatalysts for overall water splitting, *Adv. Funct, Mater.*, 2017, **27**, 1606585.

[31] S. Wang, L. Xu, W. Lu, Synergistic effect: Hierarchical Ni_3S_2@$Co(OH)_2$ heterostructure as efficient bifunctional electrocatalyst for overall water splitting, *Appl. Surf. Sci.*, 2018, **457**, 156-163.

[32] C. Du, Y. Men, X. Hei, J. Yu, G. Cheng, W. Luo, Mo-doped Ni_3S_2 nanowires as high-performance electrocatalysts for overall water splitting, *ChemElectroChem*, 2018, **5**, 2564-2570.

[33] C. H. Zhan, Z. Liu, Y. Zhou, M. L. Guo, X. L. Zhang, J. C. Tu, L. Ding, Y. Cao, Triple hierarchy and double synergies of NiFe/Co_9S_8/carbon cloth: a new and efficient electrocatalyst for the oxygen evolution reaction, *Nanoscale*, 2019, **11(7)**, 3378-3385.

[34] X. Yuan, J. Yin, Z. Liu, X. Wang, C. Dong, W. Dong, M. S. Riaz, Z. Zhang, M. Y. Chen, F. Huang, Charge transfer promoted high oxygen evolution activity of Co@Co9S8 core-shell nanochains. *ACS Appl. Mater. Interf.*, 2018, *10(14)*, 11565-11571.

[35] F. Urbain, R. F. Du, P. Y. Tang, V. Smirnov, T. Andreu, F. Finger, N. J. Divins, J. Llorcs, J. Arbiol, A. Cabot, J. R. Morante, Upscaling high activity oxygen evolution catalysts based on $CoFe_2O_4$ nanoparticles supported on nickel foam for power-to-gas electrochemical conversion with energy efficiencies above 80%, *Appl. Catal. B-Environ.*, 2019, **259**, 118055.

[36] H. Xu, J. Wei, M. Zhang, J. Wang, Y. Shiraishi, L. Tian, Y. Du, Self-supported nickel-cobalt nanowires as highly efficient and stable electrocatalysts for overall water splitting, *Nanoscale*, 2018, **10**, 18767-18773.

[37] Y. Gong, Z. Yang, Y. Lin, J. Wang, H. Pan, Z. Xu, Hierarchical heterostructure $NiCo_2O_4$@$CoMoO_4$/NF as an efficient bifunctional electrocatalyst for overall water splitting, *J. Mater. Chem. A*, 2018, **6**, 16950-16958.

[38] K. L. Wu, Z. Chen, W. C. Cheong, S. J. Liu, W. Zhu, X. Cao, K. A. Sun, Y. Lin, L. R. Zheng, W. S. Yan, Y. Pan, D. S. Wang, Q. Peng, C. Chen, Y. D. Li, Toward bifunctional overall water splitting electrocatalyst: General preparation of transition metal phosphide nanoparticles decorated N-doped porous carbon spheres, *ACS Appl. Mate. Interf.*, 2018, **10(51)**, 44201-44208.

[39] C. Tang, R. Zhang, W. Lu, L. He, X. Jiang, A. M. Asiri, X. Sun, Fe-doped CoP nanoarray: A monolithic multifunctional catalyst for highly efficient hydrogen generation, *Adv. Mater.*, 2017, **29**, 1602441.

[40] J. F. Chang, Y. Xiao, M. L. Xiao, J. J. Ge, C. P. Liu, W. Xing, Surface oxidized cobalt-phosphide nanorods as an advanced oxygen evolution catalyst in alkaline solution, *ACS Catal.*, 2015, **5(11)**, 6874-6878.

[41] C. Guan, W. Xiao, H. J. Wu, X. M. Liu, W. J. Zang, H. Zhang, J. Ding, Y. P. Feng, S. J. Pennycook, J. Wang, Hollow Mo-doped CoP nanoarrays for efficient overall water splitting, *Nano Energy*, 2018, 73-80.

[42]